

Article

Co/SiO₂ Catalyst for Methoxycarbonylation of Acetylene: On Catalytic Performance and Active Species

 An Wang ^{1,2}, Hongchen Cao ^{1,2}, Leilei Zhang ¹ and Aiqin Wang ^{1,*} 

¹ CAS Key Laboratory of Science and Technology on Applied Catalysis, iChEM, Dalian Institute of Chemical Physics, Chinese Academy of Sciences, Dalian 116023, China; wangan@dicp.ac.cn (A.W.); hongchencao@dicp.ac.cn (H.C.); zhangleilei@dicp.ac.cn (L.Z.)

² University of Chinese Academy of Sciences, Beijing 100049, China

* Correspondence: aqwang@dicp.ac.cn

Abstract: Reppe carbonylation of acetylene is an atom-economic and non-petroleum approach to synthesize acrylic acid and acrylate esters, which are key intermediates in the textile, leather finishing, and polymer industries. In the present work, a noble metal-free Co@SiO₂ catalyst was prepared and evaluated in the methoxycarbonylation reaction of acetylene. It was discovered that pretreatment of the catalyst by different reductants (i.e., C₂H₂, CO, H₂, and syngas) greatly improved the catalytic activity, of which Co/SiO₂-H₂ demonstrated the best performance under conditions of 160 °C, 0.05 MPa C₂H₂, 4 MPa CO, and 1 h, affording a production rate of 4.38 g_{MA+MP} g_{cat}⁻¹ h⁻¹ for methyl acrylate (MA) and methyl propionate (MP) and 0.91 g_{DMS} g_{cat}⁻¹ h⁻¹ for dimethyl succinate (DMS), respectively. Transmission electron microscopy (TEM), X-ray diffraction (XRD), and diffuse reflectance infrared Fourier transform spectra of CO adsorption (CO-DRIFTS) measurements revealed that an H₂ reduction decreased the size of the Co nanoparticles and promoted the formation of hollow architectures, leading to an increase in the metal surface area and CO adsorption on the catalyst. The hot filtration experiment confirmed that Co₂(CO)₈ was generated in situ during the reaction or at the pre-activation stage, which served as the genuine active species. Our work provides a facile and convenient approach to the in situ synthesis of Co₂(CO)₈ for a Reppe carbonylation reaction.

Keywords: methoxycarbonylation of acetylene; noble metal-free; cobalt carbonyls; Co leaching



Citation: Wang, A.; Cao, H.; Zhang, L.; Wang, A. Co/SiO₂ Catalyst for Methoxycarbonylation of Acetylene: On Catalytic Performance and Active Species. *Molecules* **2024**, *29*, 1987. <https://doi.org/10.3390/molecules29091987>

Academic Editors: Luísa Margarida Martins and Isidro M. Pastor

Received: 14 March 2024

Revised: 18 April 2024

Accepted: 22 April 2024

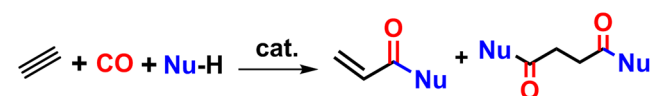
Published: 26 April 2024



Copyright: © 2024 by the authors. Licensee MDPI, Basel, Switzerland. This article is an open access article distributed under the terms and conditions of the Creative Commons Attribution (CC BY) license (<https://creativecommons.org/licenses/by/4.0/>).

1. Introduction

Reppe carbonylation reactions of acetylene (including hydrocarboxylation, alkoxy-carbonylation, etc.) (Scheme 1) provide atom-economic and non-petroleum routes to produce acrylic acid (AA), methyl acrylate, and dimethyl succinate [1,2], which are raw materials and key intermediates that are widely used in the textile, leather finishing, and polymer industries, with a global demand of 10 million tons annually [3–5].



(Nu = nucleophile, such as HO⁻, CH₃O⁻, etc)

Scheme 1. Reppe carbonylation reactions of acetylene.

Various catalysts have been developed for the carbonylation reactions of acetylene, of which Ni-based catalysts are the original ones [6]. Reppe and coworkers were the first to discover that Ni(CO)₄ was able to catalyze the hydrocarboxylation of acetylene to produce AA under 3 MPa CO and acetylene (1/1, v/v) [2]. Following this, other nickel catalysts, such as (copper-promoted) nickel halides [7,8], nickel acetates [9], and Ni-P complexes [10], were

also reported. Among others, Badische Anilin-und-Soda-Fabrik (BASF) developed the commercial catalytic system $\text{NiBr}_2\text{-CuBr}_2\text{-CH}_3\text{SOOOH}$ for hydrocarbonylation of acetylene [11], which, however, suffers from a difficulty in the separation of catalyst products [12]. To tackle this problem, metal oxides (such as SiO_2 , Al_2O_3 , vermiculite, and MCM-41) [13–15] and zeolites (e.g., NaY and ZSM-5) [16] were applied as support materials of Ni. However, these catalysts have one or more drawbacks, which include a short catalyst lifetime, harsh reaction conditions, and metal leaching. For example, Shi and coworkers reported that Ni/Y served as an efficient catalyst for the hydrocarboxylation of acetylene [17], and the AA space-time yield reached $62 \text{ g}_{\text{acrylic acid}} \text{ g}_{\text{cat}}^{-1} \text{ h}^{-1}$ under reaction conditions of $235 \text{ }^\circ\text{C}$ and 3.6 MPa . Although they claimed that the catalysis followed a heterogeneous pathway, the Ni/Y material suffered from severe coking. Yan and coworkers prepared a NiO/AlOOH catalyst, which gave an AA space-time yield as high as $412 \text{ g}_{\text{acrylic acid}} \text{ g}_{\text{cat}}^{-1} \text{ h}^{-1}$, yet it was discovered that the leached Ni-carbonyls were the true active species [12]. Given the high toxicity and instability of $\text{Ni}(\text{CO})_4$, which might generate in situ during a reaction, the potential application of Ni-based catalysts is limited.

Other catalysts based on group VIII transition metals, such as Pd, Ir, and Ru, have also been explored [18]. For instance, Drent and coworkers developed a Pd complex with the ligand of 2-pyridylphosphine (2-PyPPh₂) [19], which exhibited excellent catalytic performance in the methoxycarbonylation of propyne, and the TOF reached as high as $40,000 \text{ h}^{-1}$ with 99.95% selectivity to methyl methacrylate. The 2-pyridyl ring was found to be crucial for the catalytic activity, which, if replaced by a phenyl or 4-pyridyl group, led to a drastic decrease in TOF. Nonetheless, strong acid promoters, e.g., p-toluenesulfonic acid, are indispensable for the reaction, which would cause serious environmental issues [20]. Ding and coworkers developed porous organic polymer-supported single-site Pd catalysts, in which the 2-pyridylphosphine ligand and p-toluenesulfonic acid were incorporated into the framework of the support [21,22], and the methoxycarbonylation reaction of acetylene was allowed to run in the absence of an extra acid promoter. However, this approach suffered from tedious procedures for the preparation of the support [23,24]. In addition, the high cost and low abundance of Pd compromised its efficiency.

Cobalt is also the metal of choice for Reppe carbonylation reactions due to its earth abundance and high catalytic activity [25–27]. Pyridine-promoted cobalt carbonyls demonstrated high efficiency in converting butadiene to adipic acid in a pilot-scale process developed by BASF [28,29]. Cobalt carbonyls were also competent catalysts in the alkoxy-carbonylation reactions of alkenes [30]. Nevertheless, to the best of our knowledge, few reports have been produced on the Co-catalyzed methoxycarbonylation of acetylene. In the present work, we prepared SiO_2 -supported Co catalysts and investigated their catalytic performance in the methoxycarbonylation of acetylene in the absence of acid promoters. It was discovered that the pre-activation atmosphere (i.e., H_2 , C_2H_2 , syngas, CO, and NH_3) had a profound impact on the catalytic activity, which increased following the trend of $\text{C}_2\text{H}_2 < \text{CO} < \text{syngas} \approx \text{H}_2$. Under reaction conditions of $160 \text{ }^\circ\text{C}$ and $0.05 \text{ MPa C}_2\text{H}_2$ and 4 MPa CO , Co/ SiO_2 exhibited high catalytic activity, leading to a production rate of $4.2 \text{ g}_{\text{MA+MP}} \text{ g}_{\text{cat}}^{-1} \text{ h}^{-1}$ for MA and MP and $0.9 \text{ g}_{\text{DMS}} \text{ g}_{\text{cat}}^{-1} \text{ h}^{-1}$ for DMS, respectively. Mechanism studies by XRD and hot filtration test revealed that Co nanoparticles underwent dynamic evolution during the reaction, where cobalt carbonyls were formed in situ and served as the genuine active species. Our work provided an approach for the in situ generation of catalytically active species for the methoxycarbonylation reaction, thus circumventing the employment of costly and unstable conventional $\text{Co}_2(\text{CO})_8$ catalysts, which are generally synthesized under harsh conditions of high temperatures and high pressures [31–33].

2. Results and Discussion

The Co/ SiO_2 catalysts were prepared by the one-pot synthetic method, followed by calcination and reduction [34]. The XRD patterns (Figure 1a) exhibited characteristic diffraction peaks of metallic Co with an fcc structure (JCPDS 00-01-1259), and the size of

the Co was calculated to be 28 nm according to the Scherrer equation [35]. No diffraction peaks ascribed to SiO₂ (JCPDS 00-33-1161) were present, probably owing to the amorphous nature of SiO₂ in the sample. The TEM images (Figure 1b) and energy-dispersive X-ray (EDX) spectra (Figure 1c) showed that Co nanoparticles were homogeneously distributed on SiO₂, most of which had an average size of 18.6 nm. However, the examination of different regions showed that there were also smaller Co nanoparticles with sizes of 1–2 nm (Figure S1). The lattice spacing was measured to be 2.07 nm and 1.93 nm (Figure 1d), corresponding to the (111) and (101) plane in fcc Co, respectively, which were in agreement with the XRD measurements.

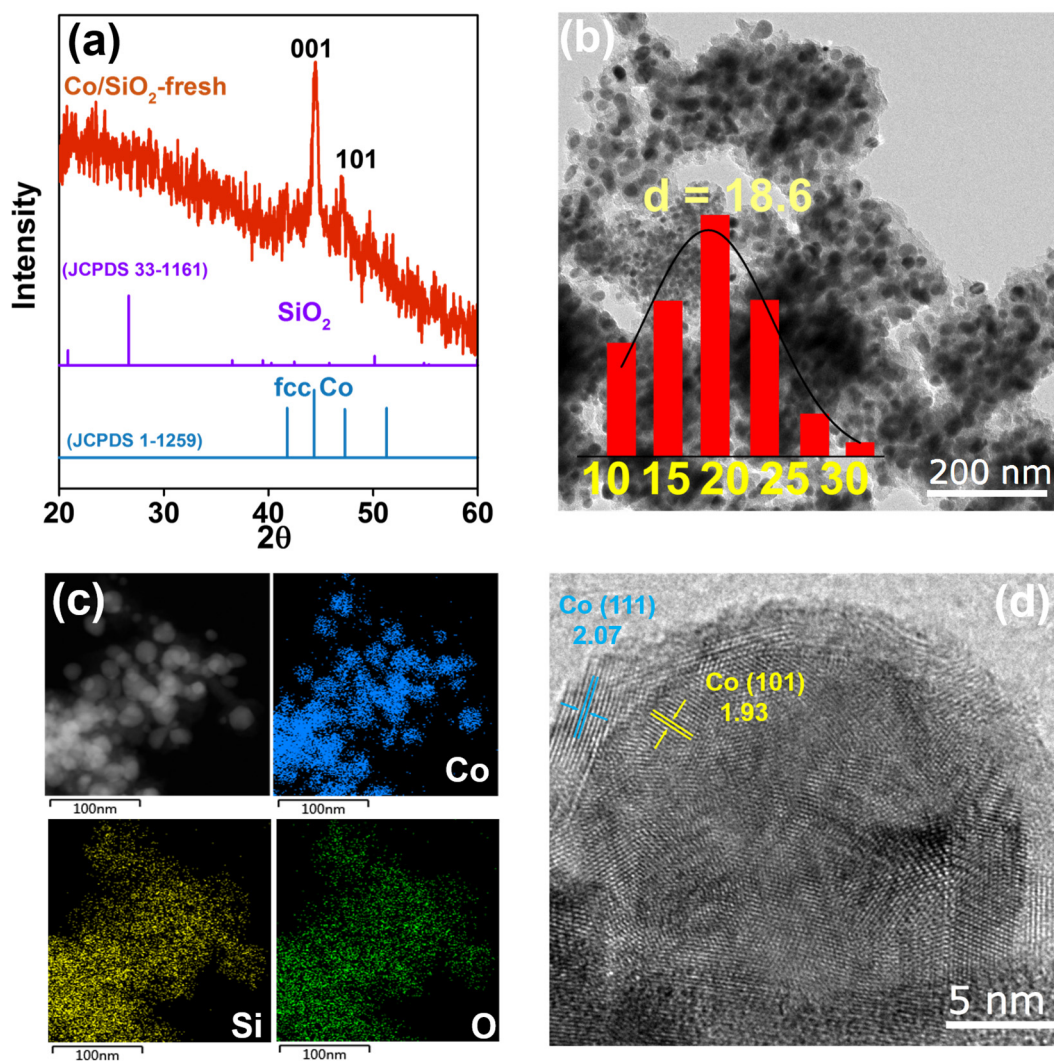


Figure 1. (a) The XRD patterns of the fresh Co/SiO₂ catalyst and the references of fcc Co and SiO₂; (b) the transmission electron microscope (TEM) images of Co/SiO₂ and the size distribution of Co nanoparticles; (c) the EDX spectra of Co, Si, and O; (d) the TEM image of Co/SiO₂ and exposed lattice plane.

The as-prepared Co/SiO₂ catalysts were evaluated in the methoxycarbonylation reaction of acetylene under conditions of 0.05 MPa C₂H₂, 4 MPa CO, 5 mL CH₃OH, and 160 °C. However, no products were detected in the three catalysts with different Co loadings after a 1 h reaction (Table 1, entries 1–3). It is assumed that the passive layer of CoO_x outside of the metallic Co might suppresses the reactant to access the catalytically active sites [36]; therefore, 1 MPa H₂ was charged into the reactor to activate the catalyst in situ. As expected, under this condition, the Co/SiO₂ samples demonstrated high catalytic performance for

the target reaction. Three main products were detected (i.e., MA, MP, and DMS) after a 1 h reaction (Table 1, entries 4–6), of which MA and DMS were produced by the methoxycarbonylation and dimethoxycarbonylation of acetylene, respectively, while MP was derived from the hydrogenation of MA. Specifically, in the 41.7% Co/SiO₂ catalyst (Table 1, entry 4), all the MA had been completely hydrogenated to MP, which was produced with a rate as high as 4.42 g_{MP} g_{cat}⁻¹ h⁻¹, and DMS was yielded with a relatively lower rate of 0.58 g_{DMS} g_{cat}⁻¹ h⁻¹. The other two Co/SiO₂ catalysts with different Co loadings were also tested in the reaction. The 31.6% Co/SiO₂ sample showed similar catalytic performance to the 41.7% Co/SiO₂ sample (Table 1, entry 5). However, the catalytic activity of the 25.6% Co/SiO₂ sample, with an even lower Co loading, decreased drastically (Table 1, entry 6), and only the methoxycarbonylation product was yielded, with a rate of 0.39 g_{MA+MP} g_{cat}⁻¹ h⁻¹. The reason might be that with a decrease in Co loading, the size of the Co became smaller, and in turn, the interaction between Co and SiO₂ became stronger (e.g., cobalt silicate might be formed) [34,37], leading to a more difficult reduction of the CoO_x species. The other support-material-loaded Co catalysts were also evaluated in the reaction. However, Co/WO_x, Co/HAP, Co/TiO₂, and Co/S-1 were totally inactive for the reaction (Table 1, entries 7–10). Metallic Co powder was inefficient for the reaction as well (Table 1, entry 11).

Table 1. Catalytic performances of various catalysts in methoxycarbonylation reaction of acetylene ^a.

Entry	Catalyst	Product Rate (g _{product} g _{cat} ⁻¹ h ⁻¹)				Yield %
		MA	MP	DMS	Others	
1	^a 41.7% Co/SiO ₂	0	0	0	0	0
2	^a 31.6% Co/SiO ₂	0	0	0	0	0
3	^a 25.6% Co/SiO ₂	0	0	0	0	0
4	^b 41.7% Co/SiO ₂	0	4.42	0.58	0.49	64.1
5	^b 31.6% Co/SiO ₂	0.43	4.0	0.56	0.39	58.6
6	^b 25.6% Co/SiO ₂	0.16	0.23	0	0	≈0
7	^b 5% Co/WO _x	0	0	0	0	0
8	^b 5% Co/HAP	0	0	0	0	0
9	^b 5% Co/TiO ₂	0	0	0	0	0
10	^b Co/S-1	0	0	0	0	0
11	^b Co powder	0	0	0	0	0

^a Reaction conditions: 10 mg catalyst, 0.05 MPa C₂H₂, 4 MPa CO, 5 mL CH₃OH, 160 °C, 1 h. ^b 0.05 MPa C₂H₂, 4 MPa CO, 1 MPa H₂, 5 mL CH₃OH, 160 °C, 1 h. Others include 1,1-dimethoxypropane (2,2-DMP) and 3-pentanone. Yield was calculated on the basis of the total amount of MA, MP, and DMS.

As the pre-activation of Co/SiO₂ by H₂ improved the catalytic activity remarkably, the other reductants, i.e., C₂H₂, CO, syngas, and NH₃, were also employed to pre-activate the sample to see if the catalytic activity could be further improved. Except for NH₃, the pre-activation was conducted in an autoclave in CH₃OH under different reductant gases at 160 °C for 1 h, and after that, the autoclave was flushed with N₂ and recharged with the reactant gas (0.05 MPa C₂H₂ and 4 MPa CO), and the reaction was allowed to run at 160 °C for 1 h. The pretreatment by NH₃ was carried out according to the literature [38]. As shown in Table 2, the pretreatment under Ar made no contribution to the activity (Table 2, entry 1), thus precluding the possibility that CH₃OH served as the reductant. By contrast, the pre-activations under C₂H₂, CO, or syngas atmosphere all led to obvious yields of the three products, and the production rate increased following the trend of Co/SiO₂-C₂H₂ (Table 2, entry 2) < Co/SiO₂-CO (entry 3) < Co/SiO₂-syngas (entry 5) ≈ Co/SiO₂-H₂ (entry 4). The improvement in catalytic activity by pretreatment with C₂H₂ or CO was surprising, as no products were detected using the as-made Co/SiO₂ catalyst under 0.05 MPa C₂H₂ and 4 MPa CO at 160 °C for 1 h, as mentioned before (Table 1, entry 1). We suppose there might be an induction period of >1 h; accordingly, the reaction was once again conducted using an as-made Co/SiO₂ catalyst under 0.05 MPa C₂H₂ and 4 MPa CO for a long time (i.e., 2 h); however, no products were detected. On the contrary,

the Co/SiO₂-NH₃ sample showed no catalytic activity for the reaction (Table 2, entry 6). The reason for this might be that NH₃ adsorbed strongly on the surface of metallic Co, and thereby, the adsorption of the reactants on the catalyst was prevented. To verify this, we carried out a control experiment, where the methoxycarbonylation of acetylene was conducted under conditions of 0.1 MPa NH₃, 0.05 MPa C₂H₂, 4 MPa CO, 5 mL CH₃OH, 160 °C, and 1 h using Co₂(CO)₈ as the catalyst (Co₂(CO)₈ was used here because it has been proven to be the genuine active species in the following section). It was found that no product was yielded, suggesting that the Co₂(CO)₈ catalyst was poisoned by NH₃.

Table 2. Catalytic performances of various pre-activated Co/SiO₂ in methoxycarbonylation reaction of acetylene ^a.

Entry	Pre-Activation	Product Rate (g _{product} g _{cat} ⁻¹ h ⁻¹)			Reaction Rate (mol _{MA+MP+DMS} mol _{Co} ⁻¹ h ⁻¹)
		MA	MP	DMS	
1	1 MPa Ar	0	0	0	0
2	0.05 MPa C ₂ H ₂	1.51	0	0.42	0.31
3	4 MPa CO	2.91	0.03	0.54	0.56
4	1 MPa H ₂	4.23	0.15	0.91	0.85
5	1 MPa H ₂ + 4 MPa CO	3.4	0.16	1.25	0.77
6	0.01 MPa NH ₃	0	0	0	0

^a Reaction conditions: 10 mg catalyst, 0.05 MPa C₂H₂, 4 MPa CO, 5 mL CH₃OH, 160 °C, 1 h.

On the basis of the above results, it is inferred that pretreatment with a distinct reducing gas should modify the structure of the Co/SiO₂ catalyst, where the active species are more prone to be formed. Accordingly, TEM, XRD, and CO-DRIFT measurements of the activated catalysts were conducted. Figure 2 shows the TEM images and particle size histograms for different pre-activated Co/SiO₂ samples. The average particle size of metallic Co was 24.9 nm, and it was 20.3 nm for Co/SiO₂-C₂H₂ (Figure 2a,d) and Co/SiO₂-CO (Figure 2b,e), respectively. Compared with fresh Co/SiO₂ (18.6 nm), it is obvious that the C₂H₂ and CO pre-activation induce an increase in particle size. In sharp contrast, in the Co/SiO₂-H₂ sample (Figure 2c,f and Figure S2), not only had the size of the Co decreased to 17.5 nm, but also, a lot of Co nanoparticles had been reconstructed to hollow shells. This reconstruction during H₂ reduction might result from the strain induced by a variation in the metal–metal distances between the CoO_x surface layer and the inner metallic Co [39].

As shown in Figure 3a, the intensity of the diffraction peaks at 44.4° and 47.3°, attributed to the (111) and (101) plane of metallic Co [40] in the samples of Co/SiO₂-C₂H₂ and Co/SiO₂-CO, increased greatly compared with those of the fresh Co/SiO₂, indicating an increase in the size of the Co nanoparticles. In sharp contrast, for the Co/SiO₂-H₂ sample, the diffraction peaks attenuated instead, suggesting a decrease in the Co particle size, or a reduction in the crystallinity of the metallic Co. These results were consistent with the TEM examination results but quite different from conventional experimental results, where H₂ reduction generally results in the sintering of metal nanoparticles [41]. CO-DRIFTS were also carried out to study the electronic properties of Co. As shown in Figure 3b, four adsorption bands appeared on different samples. The band at 2048 cm⁻¹ was ascribed to the ν(C≡O) of CO molecules that were linearly adsorbed on metallic Co [42], while the one at 1793 cm⁻¹ was assigned to the ν(C≡O) of CO molecules in multi-bonded carbonyls on Co [43]. The other two bands at 1627 and 1510 cm⁻¹ were attributed to the ν_{asymm}(C=O) of bicarbonate species and ν_{asymm}(C=O) of carbonate species, respectively [44,45]. It was found that the integrated area of the CO band at 2048 cm⁻¹ and 1793 cm⁻¹ increased with the trend of Co/SiO₂-C₂H₂ < Co/SiO₂-CO < Co/SiO₂-H₂, indicating an increased surface area of the metallic Co, which should come from the reduction of the passive layer of CoO_x. In addition, this peak red-shifted to 2030 cm⁻¹ on Co/SiO₂-CO and further to 2019 cm⁻¹ on Co/SiO₂-H₂, which, according to the TEM images, might result from the increased proportion of corner and edge sites in the Co nanoparticles with a decrease in sizes.

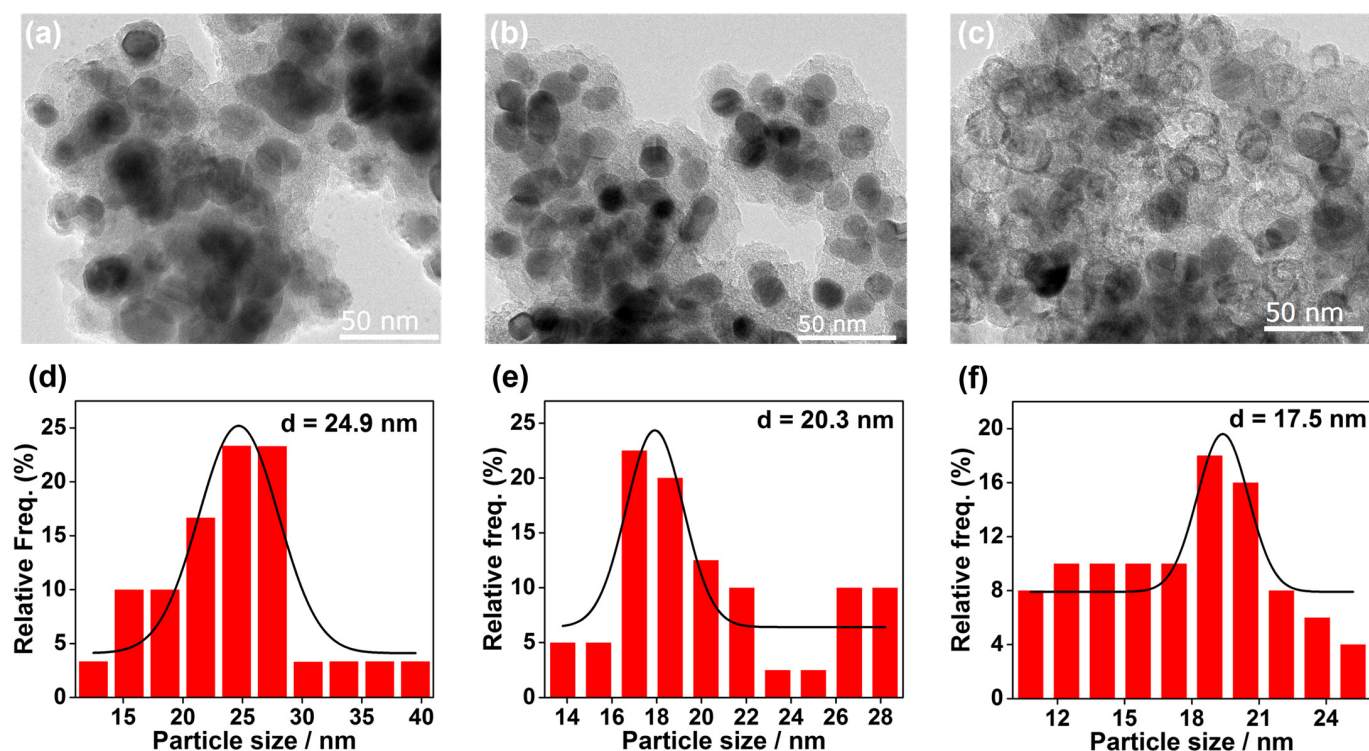


Figure 2. Representative TEM images and corresponding particle size histograms for pre-activated catalysts: (a,d) Co/SiO₂-C₂H₂; (b,e) Co/SiO₂-CO; (c,f) Co/SiO₂-H₂.

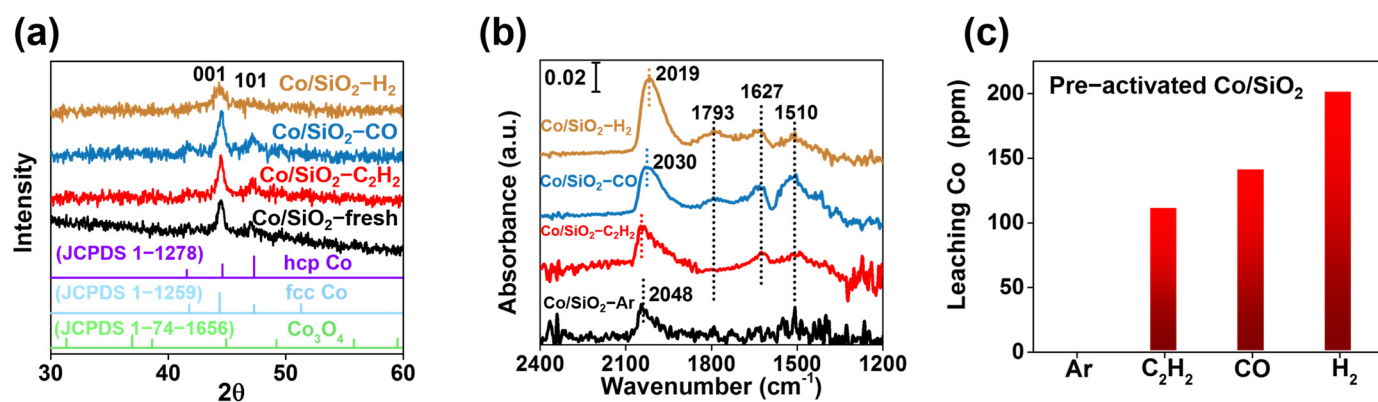


Figure 3. (a) XRD patterns of fresh and pre-activated Co/SiO₂, as well as reference Co samples; (b) DRIFT spectra of CO adsorption on different samples; (c) amount of leaching Co in reaction filtrate from pre-activated Co/SiO₂ (determined by ICP-OES).

Stability is a key criterion for judging the quality of a catalyst [46]. Therefore, we also studied the recyclability of the Co/SiO₂ catalyst. When the used catalyst was separated from the reaction mixture by filtration, it was found that the filtrate was dark red in color, suggesting severe leaching of Co [47,48]. The concentration of Co in the filtrate of different samples increased, following the trend of Co/SiO₂-C₂H₂ < Co/SiO₂-CO < Co/SiO₂-H₂ (Figure 3c), which was in agreement with that of the catalytic activity. In addition, the Co/SiO₂ catalyst was discovered to already undergo Co leaching after the pretreatment with the reductant. In particular, for the Co/SiO₂-syngas sample, after the pre-activation using syngas, the solid sample was separated by filtration and was then subjected to a batch of reactions (Figure S4); however, no products were yielded at all. By contrast, when the dark-red filtrate (containing 200 ppm Co) was employed as a catalyst, production rates of 3.76 g_{MA+MP} g_{cat}⁻¹ h⁻¹ of MA and MP and 0.49 g_{DMS} g_{cat}⁻¹ h⁻¹ of DMS were

achieved (Table 3), which was quite similar to that of the Co/SiO₂-syngas (Table 2, entry 5). These results indicated that it was the leached Co species that contributed to the overall catalytic activity. ¹³C NMR measurement was then conducted to identify the leached Co species; however, the filtrate did not show any signal because of the paramagnetic nature of Co. The yellow color of the filtrate implied that the leached Co species might be Co₂(CO)₈. To confirm this point, we used commercial Co₂(CO)₈ as a catalyst for the methoxycarbonylation of acetylene. It was discovered that Co₂(CO)₈ demonstrated similar catalytic activity and product distribution to the filtrate (Figure 4), verifying that Co₂(CO)₈ was the true active species for the reaction.

Table 3. Catalytic performances of filtrate and residual solids in methoxycarbonylation reaction of acetylene ^a.

Catalyst	Product Rate (g _{product} g _{cat} ⁻¹ h ⁻¹)		
	MA	MP	DMS
^a Filtrate	3.6	0.16	0.35
^a Residual solid	0	0	0

^a Reaction conditions: 10 mg catalyst, 0.05 MPa C₂H₂, 4 MPa CO, 5 mL CH₃OH, 160 °C, 1 h.

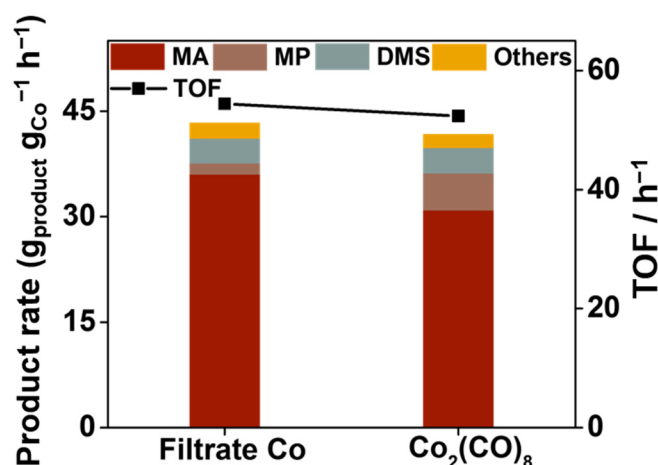


Figure 4. Catalytic performances in methoxycarbonylation of acetylene using Co leaching and Co₂(CO)₈. Reaction conditions: 2.89 mg Co₂(CO)₈, 0.05 MPa C₂H₄, 4 MPa CO, 5 mL CH₃OH, 160 °C, 1 h; for filtrate Co, there are 200 ppm Co in solution.

Co₂(CO)₈ is known as an efficient catalyst for the alkoxy carbonylation and hydroformylation of alkenes [49–51], although no reports on its catalytic performance in the methoxycarbonylation of acetylene have been published. Our work thus demonstrated that Co₂(CO)₈ is also a competent catalyst for this transformation to produce MA and MP. Traditionally, Co₂(CO)₈ is quite unstable, and its synthesis requires either harsh reaction conditions (i.e., 140–230 °C, 10–70 MPa) or stoichiometric reducing reagents (such as metal powders, NaBH₄, or Na₂S₂SO₃) or phosphine oxide promoters. Li and coworkers recently reported that Co₂(CO)₈ could be formed in situ from Co/MoS₂ under conditions of 6 MPa CO, 140 °C, and 15 h, and MoS₂ was claimed to be critical for this process [28]. This work demonstrated that when using conventional SiO₂ as a support material, Co₂(CO)₈ could also be generated in situ under conditions of 4 MPa CO, 1 MPa H₂, 160 °C, and 1 h, thus providing a facile, straightforward approach to prepare Co₂(CO)₈ for Reppe carbonylation reactions.

3. Materials and Methods

The Co/SiO₂ was prepared according to the literature [34]. Briefly, 2.91 g Co(NO₃)₂·6H₂O (10 mmol) and 2.08 g TEOS (10 mmol) were dissolved in 50 mL mixed liquor of water and

ethanol (3/1, *v/v*) and stirred for 10 min. After, 5 mL of $\text{NH}_3 \cdot \text{H}_2\text{O}$ was added to the above solution, and the suspension was stirred at room temperature for another 8 h. The precipitate was separated and collected by filtration, washed with deionized water, and dried at 100 °C overnight. The obtained solid was calcined at 500 °C in a muffle furnace for 4 h and was then reduced in flowing pure hydrogen (100 mL/min) for 3 h at 600 °C. The obtained Co/SiO₂ catalyst was labeled as 41.7% Co/SiO₂. The other two catalysts with different Co loadings (i.e., 31.6% Co/SiO₂ and 25.6% Co/SiO₂) were prepared using similar procedures, except for changing the amount of TEOS to 15 and 20 mmol, respectively.

The other support material (i.e., WO_x, hydroxyapatite (HAP), and TiO₂)-loaded Co catalysts were synthesized by the impregnation method. First, 5 mL $\text{Co}(\text{NO}_3)_2 \cdot 6\text{H}_2\text{O}$ solution (10 mg Co/mL) and 5 mL ultrapure water were mixed and stirred to form a transparent solution, and then, 1 g carrier was added to the above solution. After the mixture was stirred at room temperature for 24 h, the excess water was removed by rotary evaporation until dry. The resulting powder was further dried at 373 K overnight and then reduced in flowing pure hydrogen (100 mL/min) for 3 h at 600 °C.

The preparation of the $\text{Co}_2(\text{CO})_8$ solution in methanol from Co/SiO₂ started with adding 10 mg of fresh Co/SiO₂ to a 30 mL autoclave with 5 mL methanol, and then, the autoclave was purged with N₂ repeatedly (4 times) to remove gaseous and dissolved oxygen. After that, the autoclave was charged with 4 MPa CO and 1 MPa H₂, and the mixture was stirred (600 rpm) at 160 °C for 4 h. Then, the autoclave was placed into an ice bath until the temperature was below 5 °C. The solid was separated by filtration, and the yellow filter liquor was collected and kept at 0 °C.

Other comparison materials, including Co powder and $\text{Co}_2(\text{CO})_8$, are commercial samples at analytically pure levels.

3.1. Characterization

The concentration of Co in the filtrate after pretreatment or reaction was determined by inductively coupled plasma spectroscopy (ICP-AES) on an IRIS Intrepid II XSP instrument (Thermo Electron Corporation, Waltham, MA, USA). The patterns of XRD were recorded on a PANalytical X'pert diffractometer with a Cu-K α radiation source, operated at 40 kV and 40 mA under a continuous mode in the 2 θ range of 10°~90°. The morphology and element distribution of samples were observed by STEM and EDS experiments, which were performed on a JEM-2100F Transmission Electron Microscope (JEOL, Singapore) with a spatial resolution of 0.19 nm at 20 kV, equipped with the Oxford Instruments ISIS/INCA EDS system with an Oxford Pentafet Ultrathin Window (UTW) detector. Before the microscopy examination, the sample was demagnetization-treated using a magnet. After that, the sample was ultrasonically dispersed in ethanol for 5–10 min, and then, a drop of the suspension was dropped on a copper TEM grid coated with a thin holey carbon film. CO-DRIFTS (diffuse reflectance infrared Fourier transform spectroscopy) experiments were performed by means of a Bruker Equinox70 spectrometer (Bruker, Singapore), equipped with a mercury–cadmium–telluride detector at a resolution of 4 cm⁻¹, using 16 scans in a range of 400–4000 cm⁻¹. Prior to the measurement, the catalysts were pretreated in situ with H₂ (30 mL/min) at 160 °C for 30 min, and then, the flow was switched to He (30 mL/min) at 170 °C for another 30 min to remove surface H. After that, the catalyst cooled down to room temperature, and background spectra were recorded at 20 °C in He flow.

3.2. Catalyst Evaluation

The acetylene methoxycarbonylation (AMC) reaction was performed in a 30 mL autoclave equipped with a quartz lining. The autoclave was filled with 10 mg of a catalyst and 5 mL methanol, and then, the autoclave was purged with N₂ repeatedly (4 times) to remove gaseous and dissolved oxygen. After that, it was charged with 1 MPa 5% C₂H₂-95% He, 1 MPa H₂, and 4 MPa CO. The reaction was started by heating the mixture to 160 °C under vigorous stirring at a speed of 600 rpm. After the reaction, the reactor was cooled to

room temperature, and the liquid product was analyzed using n-pentanol as the internal by gas chromatography (Agilent 7890B, Santa Clara, CA, USA), equipped with an HP-INNO WAX column (30 m × 320 μm × 0.25 μm). Only methyl acrylate (MA), methyl propionate (MP), dimethyl succinate (DMS), 1,1-dimethoxypropane (2,2-DMP), and 3-pentanone were detected in the liquid product. The reaction selectivity was calculated based on the molar ratio of MA, MP, and DMS to the total liquid product, and the reaction rate was calculated by the total mass of MA, MP, and DMS produced per mass of Co per hour. The ‘others’ in the result are the total mass of 3-pentanone and 2,2-DMP. It should be emphasized when using $\text{Co}_2(\text{CO})_8$ as a catalyst before the reactant gas is charged that the autoclave should be placed into an ice bath until the temperature is below 5 °C; otherwise, the dissolved $\text{Co}_2(\text{CO})_8$ will be swept away owing the volatile property of $\text{Co}_2(\text{CO})_8$.

The pretreatment of the Co/SiO₂ catalyst and the catalytic evaluation were conducted in a methoxycarbonylation reaction of acetylene. Taking Co/SiO₂-C₂H₂ as an example, 10 mg of fresh Co/SiO₂ was added into a 30 mL autoclave with 5 mL methanol, and then, the autoclave was purged with N₂ repeatedly (4 times) to remove the air and dissolved oxygen. After that, the autoclave was charged with 5% C₂H₂-95% He until 1 MPa. The autoclave was heated at 160 °C for 1 h with vigorous stirring at a speed of 600 rpm. When the reactor was cooled to room temperature, the gas in the reactor was evacuated, and the autoclave was recharged with C₂H₂ (1 MPa) and CO (4 MPa) for acetylene methoxycarbonylation. A similar pretreatment process was also conducted using 1 MPa H₂, 4 MPa CO, or syngas (a mixture of 1 MPa H₂ and 4 MPa CO).

4. Conclusions

In summary, a noble metal-free Co@SiO₂ catalyst was prepared and tested in the methoxycarbonylation reaction of acetylene. The pre-activation of the catalyst using different reductant gases (i.e., C₂H₂, CO, H₂, and syngas) was found to be crucial for the high catalytic performance. The catalytic activity increased following the trend of Co/SiO₂-C₂H₂ < Co/SiO₂-CO < Co/SiO₂-syngas ≈ Co/SiO₂-H₂, and high production rates of 4.38 g_{MA+MP} g_{cat}⁻¹ h⁻¹ and 0.91 g_{DMS} g_{cat}⁻¹ h⁻¹ were obtained for Co/SiO₂-H₂ under conditions of 160 °C, 0.05 MPa C₂H₂, 4 MPa CO, and 1 h. The characterization by TEM, XRD, and CO-DRIFTS revealed that the size or crystallinity of Co nanoparticles was greatly decreased upon pre-reduction by H₂, which remarkably increased the metal surface area and CO adsorption on the catalyst. The hot filtration experiment and controlled measurement confirmed that Co was leached into the solution in the form of $\text{Co}_2(\text{CO})_8$ and served as the genuine active species. Our work provides a facile and convenient approach to synthesize $\text{Co}_2(\text{CO})_8$ for a Reppe carbonylation reaction, thus avoiding the direct usage of highly costly and unstable $\text{Co}_2(\text{CO})_8$ as a catalyst.

Supplementary Materials: The following supporting information can be downloaded at <https://www.mdpi.com/article/10.3390/molecules29091987/s1>: Figure S1: STEM images of Co/SiO₂ at different magnifications; Figure S2: (a–c) TEM images of pre-activated Co/SiO₂-H₂; Figure S3: DRIFT spectra of CO adsorption on different samples; Figure S4: Diagram illustration of separation process.

Author Contributions: Conceptualization, A.W. (Aiqin Wang) and L.Z.; methodology, A.W. (An Wang); investigation, A.W. (An Wang) and H.C.; writing—original draft preparation, A.W. (An Wang); writing—review and editing, L.Z.; supervision, A.W. (Aiqing Wang). All authors have read and agreed to the published version of the manuscript.

Funding: This research was funded by the National Key R&D Program of China (2023YFA1506603), the NSFC Center for Single-atom Catalysis (Grant NO. 22388102), National Natural Science Foundation of China (22132006, 22172159), the CAS Project for Young Scientists in Basic Research (YSBR-022), and the Youth Innovation Promotion Association CAS (2022185).

Institutional Review Board Statement: Not applicable.

Informed Consent Statement: Not applicable.

Data Availability Statement: Data are contained within the article and Supplementary Materials.

Conflicts of Interest: The authors declare no conflicts of interest.

References

1. Kiss, G. Palladium-catalyzed Reppe carbonylation. *Chem. Rev.* **2001**, *101*, 3435–3456. [[CrossRef](#)]
2. Trotus, I.T.; Zimmermann, T.; Schueth, F. Catalytic Reactions of Acetylene: A Feedstock for the Chemical Industry Revisited. *Chem. Rev.* **2014**, *114*, 1761–1782. [[CrossRef](#)] [[PubMed](#)]
3. Kalck, P.; Urrutigoity, M. Recent improvements in the alkoxycarbonylation reaction catalyzed by transition metal complexes. *Inorg. Chim. Acta* **2015**, *431*, 110–121. [[CrossRef](#)]
4. Chinchilla, R.; Nájera, C. Chemicals from Alkynes with Palladium Catalysts. *Chem. Rev.* **2014**, *114*, 1783–1826. [[CrossRef](#)] [[PubMed](#)]
5. Li, X.J.; Wang, J.Q.; Yuan, Q.; Song, X.E.; Mu, J.L.; Wei, Y.; Yan, L.; Sun, F.F.; Feng, S.Q.; Cai, Y.T.; et al. Palladium and Ruthenium Dual-Single-Atom Sites on Porous Ionic Polymers for Acetylene Dialkoxycarbonylation: Synergetic Effects Stabilize the Active Site and Increase CO Adsorption. *Angew. Chem. Int. Ed.* **2023**, *62*, 202307570. [[CrossRef](#)] [[PubMed](#)]
6. Reppe, W. New developments in the field of chemical acetylene and coal. *Experientia* **1949**, *5*, 93–110. [[CrossRef](#)]
7. Bhattacharyya, S.K.; Sen, A.K. Catalytic Syntheses of Acrylic Acid and Ethyl Acrylate from Acetylene, Carbon Monoxide, and Water or Ethanol under Pressure. *Ind. Eng. Chem. Process Des. Dev.* **1964**, *3*, 169–176. [[CrossRef](#)]
8. Bhattacharyya, S.K.; Nag, S.N. Catalytic synthesis of ethyl propionate from ethylene, carbon monoxide and ethanol at high pressure. *J. Appl. Chem.* **1962**, *12*, 182. [[CrossRef](#)]
9. Cui, L.; Yang, X.G.; Zeng, Y.; Chen, Y.T.; Wang, G.Y. A unique nickel-base nitrogen-oxygen bidentate ligand catalyst for carbonylation of acetylene to acrylic acid. *Mol. Catal.* **2019**, *468*, 57–61. [[CrossRef](#)]
10. Tang, C.M.; Zeng, Y.; Cao, P.; Yang, X.G.; Wang, G.Y. The Nickel and Copper-Catalyzed Hydroformylation of Acetylene with Carbon Monoxide to Acrylic Acid. *Catal. Lett.* **2009**, *129*, 189–193. [[CrossRef](#)]
11. Lin, T.J.; Meng, X.; Shi, L. Catalytic hydrocarboxylation of acetylene to acrylic acid using Ni₂O₃ and cupric bromide as combined catalysts. *J. Mol. Catal. A Chem.* **2015**, *396*, 77–83. [[CrossRef](#)]
12. Li, Y.K.; Yan, L.F.; Zhang, Q.F.; Yan, B.H.; Cheng, Y. A recyclable heterogeneous-homogeneous-heterogeneous NiO/AlOOH catalysis system for hydrocarboxylation of acetylene to acrylic acid. *RSC Adv.* **2020**, *10*, 1634–1638. [[CrossRef](#)] [[PubMed](#)]
13. Bhattacharyya, S.K.; Bhattach, D.P. Catalytic synthesis of n-propyl acrylate from acetylene carbon monoxide and n-propanol under pressure. *J. Appl. Chem.* **1966**, *16*, 18. [[CrossRef](#)]
14. Hu, G.; Guo, D.; Shang, H.J.; Sun, Y.K.; Zeng, J.M.; Li, J.B.; Zhu, M.Y. Expanded Two-Dimensional Layered Vermiculite Supported Nickel Oxide Nanoparticles Provides High Activity for Acetylene Carbonylation to Synthesize Acrylic Acid. *Catal. Lett.* **2020**, *150*, 674–682. [[CrossRef](#)]
15. Hu, G.; Guo, D.; Shang, H.J.; Sun, Y.K.; Zeng, J.M.; Li, J.B. Microwave-Assisted Rapid Preparation of Vermiculite-Loaded Nano-Nickel Oxide As a Highly Efficient Catalyst for Acetylene Carbonylation to Synthesize Acrylic Acid. *Chem. Select.* **2020**, *5*, 2940–2948. [[CrossRef](#)]
16. Xie, H.; Lin, T.J.; Shi, L.; Meng, X. Acetylene carbonylation over Ni-containing catalysts: Role of surface structure and active site distribution. *RSC Adv.* **2016**, *6*, 97285–97292. [[CrossRef](#)]
17. Lin, T.J.; Meng, X.; Shi, L. Ni-exchanged Y-zeolite. An efficient heterogeneous catalyst for acetylene hydrocarboxylation. *Appl. Catal. A* **2014**, *485*, 163–171. [[CrossRef](#)]
18. Wu, X.F.; Fang, X.J.; Wu, L.P.; Jackstell, R.; Neumann, H.; Beller, M. Transition-Metal-Catalyzed Carbonylation Reactions of Olefins and Alkynes: A Personal Account. *Acc. Chem. Res.* **2014**, *47*, 1041–1053. [[CrossRef](#)] [[PubMed](#)]
19. Drent, E.; Arnoldy, P.; Budzelaar, P.H.M. Homogeneous catalysis by cationic palladium complexes precision catalysis in the carbonylation of alkynes. *J. Organomet. Chem.* **1994**, *475*, 57–63. [[CrossRef](#)]
20. Wei, X.M.; Ma, Z.W.; Mu, X.Y.; Lu, J.Z.; Hu, B. Catalyst in Acetylene Carbonylation: From Homogeneous to Heterogeneous. *Prog. Chem.* **2021**, *33*, 243–253. [[CrossRef](#)]
21. Chen, X.K.; Zhu, H.J.; Wang, W.L.; Du, H.; Wang, T.; Yan, L.; Hu, X.P.; Ding, Y.J. Multifunctional Single-Site Catalysts for Alkoxycarbonylation of Terminal Alkynes. *ChemSusChem* **2016**, *9*, 2451–2459. [[CrossRef](#)] [[PubMed](#)]
22. Chen, X.K.; Zhu, H.J.; Wang, T.; Li, C.Y.; Yan, L.; Jiang, M.; Liu, J.; Sun, X.P.; Jiang, Z.; Ding, Y.J. The 2V-P,N polymer supported palladium catalyst for methoxycarbonylation of acetylene. *J. Mol. Catal. A Chem.* **2016**, *414*, 37–46. [[CrossRef](#)]
23. Wang, A.; Zhang, L.L.; Yu, Z.A.; Zhang, S.X.; Li, L.; Ren, Y.J.; Yang, J.; Liu, X.Y.; Liu, W.; Yang, X.F.; et al. Ethylene Methoxycarbonylation over Heterogeneous Pt₁/MoS₂ Single-Atom Catalyst: Metal-Support Concerted Catalysis. *J. Am. Chem. Soc.* **2023**, *146*, 695–706. [[CrossRef](#)] [[PubMed](#)]
24. Li, X.J.; Feng, S.Q.; Hemberger, P.; Bodi, A.; Song, X.G.; Yuan, Q.; Mu, J.L.; Li, B.; Jiang, Z.; Ding, Y.J. Iodide-Coordinated Single-Site Pd Catalysts for Alkyne Dialkoxycarbonylation. *ACS Catal.* **2021**, *11*, 9242–9251. [[CrossRef](#)]
25. Sarkar, B.R.; Chaudhari, R.V. Carbonylation of alkynes, alkenes and alcohols using metal complex catalysts. *Catal. Surv. Asia* **2005**, *9*, 193–205. [[CrossRef](#)]
26. Zhang, X.H.; Shen, C.R.; Xia, C.G.; Tian, X.X.; He, L. Alkoxycarbonylation of olefins with carbon dioxide by a reusable heterobimetallic ruthenium-cobalt catalytic system. *Green Chem.* **2018**, *20*, 5533–5539. [[CrossRef](#)]

27. Pesa, F.; Haase, T. The cobalt-catalyzed hydroesterification of acrylonitrile. *J. Mol. Catal.* **1983**, *18*, 237–249. [[CrossRef](#)]
28. Zheng, Z.; Zhou, H.; Deng, L.; Jia, X.; Li, Y. Molybdenum disulfide promoted co-catalyzed alkoxycarbonylation. *J. Catal.* **2024**, *430*, 115349. [[CrossRef](#)]
29. Hofmann, P.; Kosswig, K.; Schaefer, W. Hydrocarboxymethylation—An attractive route from olefins to fatty-acid esters? *Ind. Eng. Chem. Prod. Res. Dev.* **1980**, *19*, 330–334. [[CrossRef](#)]
30. Huang, W.H.; Jackstell, R.; Spannenberg, A.; Beller, M. An improved cobalt-catalysed alkoxycarbonylation of olefins using secondary phosphine oxide promoters. *Catal. Sci. Technol.* **2023**, *13*, 2475–2479. [[CrossRef](#)]
31. Orchin, M. Hydrogenation of organic compounds with synthesis gas. *Adv. Catal.* **1953**, *5*, 385–415. [[CrossRef](#)]
32. Satyanarayana, N.; Periasamy, M. Carbonylation of benzyl halides using $\text{CoCl}_2/\text{NaBH}_4/\text{CO}/\text{NaOH}$ reagent system. *Tetrahedron Lett.* **1987**, *28*, 2633–2636. [[CrossRef](#)]
33. Itoh, K.; Miura, M.; Nomura, M. Normal pressure double carbonylation of aryl halides using Cobalt(ii) chloride in the presence of either sodium sulfide or sodium-borohydride. *Bull. Chem. Soc. Jpn.* **1988**, *61*, 4151–4152. [[CrossRef](#)]
34. Wang, L.X.; Guan, E.J.; Wang, Y.Q.; Wang, L.; Gong, Z.M.; Cui, Y.; Meng, X.J.; Gates, B.C.; Xiao, F.S. Silica accelerates the selective hydrogenation of CO_2 to methanol on cobalt catalysts. *Nat. Commun.* **2020**, *11*, 14817. [[CrossRef](#)] [[PubMed](#)]
35. Muniz, F.T.L.; Miranda, M.A.R.; dos Santos, C.M.; Sasaki, J.M. The Scherrer equation and the dynamical theory of X-ray diffraction. *Acta Crystallogr. Sect. A Found. Adv.* **2016**, *72*, 385–390. [[CrossRef](#)] [[PubMed](#)]
36. Kaneti, Y.V.; Zhang, J.; He, Y.B.; Wang, Z.J.; Tanaka, S.; Hossain, M.S.A.; Pan, Z.Z.; Xiang, B.; Yang, Q.H.; Yamauchi, Y. Fabrication of an MOF-derived heteroatom-doped Co/CoO/carbon hybrid with superior sodium storage performance for sodium-ion batteries. *J. Mater. Chem.* **2017**, *5*, 15356–15366. [[CrossRef](#)]
37. Zhang, Q.H.; Deng, W.P.; Wang, Y. Recent advances in understanding the key catalyst factors for Fischer-Tropsch synthesis. *J. Energy Chem.* **2013**, *22*, 27–38. [[CrossRef](#)]
38. Guan, D.Q.; Zhong, J.; Xu, H.Y.; Huang, Y.C.; Hu, Z.W.; Chen, B.; Zhang, Y.; Ni, M.; Xu, X.M.; Zhou, W.; et al. A universal chemical-induced tensile strain tuning strategy to boost oxygen-evolving electrocatalysis on perovskite oxides. *Appl. Phys. Res.* **2022**, *9*, 011422. [[CrossRef](#)]
39. LaGrow, A.P.; Lloyd, D.C.; Gai, P.L.; Boyes, E.D. In Situ Scanning Transmission Electron Microscopy of Ni Nanoparticle Redispersion via the Reduction of Hollow NiO. *Chem. Mater.* **2018**, *30*, 197–203. [[CrossRef](#)]
40. Du, H.; Jiang, M.; Zhu, H.J.; Huang, C.D.; Zhao, Z.; Dong, W.D.; Lu, W.; Liu, T.; Zhang, Z.C.; Ding, Y.J. Constructing efficient hcp-Co active sites for Fischer-Tropsch reaction on an activated carbon supported cobalt catalyst via multistep activation processes. *Fuel* **2021**, *292*, 120244. [[CrossRef](#)]
41. Parastayev, A.; Muravev, V.; Osta, E.H.; van Hoof, A.J.F.; Kimpel, T.F.; Kosinov, N.; Hensen, E.J.M. Boosting CO_2 hydrogenation via size-dependent metal-support interactions in cobalt/ceria-based catalysts. *Nat. Catal.* **2020**, *3*, 526–533. [[CrossRef](#)]
42. Parastayev, A.; Muravev, V.; Osta, E.H.; Kimpel, T.F.; Simons, J.F.M.; van Hoof, A.J.F.; Uslamin, E.; Zhang, L.; Struijs, J.J.C.; Burueva, D.B.; et al. Breaking structure sensitivity in CO_2 hydrogenation by tuning metal-oxide interfaces in supported cobalt nanoparticles. *Nat. Catal.* **2022**, *5*, 1051–1060. [[CrossRef](#)]
43. Weststrate, C.J.; van de Loosdrecht, J.; Niemantsverdriet, J.W. Spectroscopic insights into cobalt-catalyzed Fischer-Tropsch synthesis: A review of the carbon monoxide interaction with single crystalline surfaces of cobalt. *J. Catal.* **2016**, *342*, 1–16. [[CrossRef](#)]
44. Zhu, H.Q.; Qin, Z.F.; Shan, W.J.; Shen, W.J.; Wang, J.G. Pd/CeO₂-TiO₂ catalyst for CO oxidation at low temperature: A TPR study with H₂ and CO as reducing agents. *J. Catal.* **2004**, *225*, 267–277. [[CrossRef](#)]
45. Tabakova, T.; Boccuzzi, F.B.; Manzoli, M.; Andreeva, D. FTIR study of low-temperature water-gas shift reaction on gold/ceria catalyst. *Appl. Catal. A* **2003**, *252*, 385–397. [[CrossRef](#)]
46. Banham, D.; Ye, S.; Pei, K.; Ozaki, J.; Kishimoto, T.; Imashiro, Y. A review of the stability and durability of non-precious metal catalysts for the oxygen reduction reaction in proton exchange membrane fuel cells. *J. Power Sources* **2015**, *285*, 334–348. [[CrossRef](#)]
47. Hertrich, M.F.; Scharnagl, F.K.; Pews-Davtyan, A.; Kreyenschulte, C.R.; Lund, H.; Bartling, S.; Jackstell, R.; Beller, M. Supported Cobalt Nanoparticles for Hydroformylation Reactions. *Chem. Eur. J.* **2019**, *25*, 5534–5538. [[CrossRef](#)]
48. Zhao, J.J.; He, Y.R.; Wang, F.; Zheng, W.T.; Huo, C.F.; Liu, X.; Jiao, H.J.; Yang, Y.; Li, Y.W.; Wen, X.D. Suppressing Metal Leaching in a Supported Co/SiO₂ Catalyst with Effective Protectants in the Hydroformylation Reaction. *ACS Catal.* **2020**, *10*, 914–920. [[CrossRef](#)]
49. Rush, L.E.; Pringle, P.G.; Harvey, J.N. Computational Kinetics of Cobalt-Catalyzed Alkene Hydroformylation. *Angew. Chem. Int. Ed.* **2014**, *53*, 8672–8676. [[CrossRef](#)]
50. Franke, R.; Selent, D.; Börner, A. Applied Hydroformylation. *Chem. Rev.* **2012**, *112*, 5675–5732. [[CrossRef](#)]
51. Hood, D.M.; Johnson, R.A.; Carpenter, A.E.; Younker, J.M.; Vinyard, D.J.; Stanley, G.G. Highly active cationic cobalt(II) hydroformylation catalysts. *Science* **2020**, *367*, 542–549. [[CrossRef](#)] [[PubMed](#)]

Disclaimer/Publisher's Note: The statements, opinions and data contained in all publications are solely those of the individual author(s) and contributor(s) and not of MDPI and/or the editor(s). MDPI and/or the editor(s) disclaim responsibility for any injury to people or property resulting from any ideas, methods, instructions or products referred to in the content.